PHYSICAL REVIEW B **85**, 121303(R) (2012)

Spin dephasing of fluorine-bound electrons in ZnSe

A. Greilich,[1,*] A. Pawlis,[2,3,†] F. Liu,[1] O. A. Yugov,[1] D. R. Yakovlev,[1,4] K. Lischka,[2] Y. Yamamoto,[3,5] and M. Bayer[1]

[1]*Experimentelle Physik 2, Technische Universität Dortmund, 44227 Dortmund, Germany*

[2]*Department Physik, Universität Paderborn, 33098 Paderborn, Germany*

[3]*Edward L. Ginzton Laboratory, Stanford University, Stanford, California 94305-4088, USA*

[4]*Ioffe Physical-Technical Institute, Russian Academy of Sciences, 194021 St. Petersburg, Russia*

[5]*National Institute of Informatics, 2-1-2 Hitotsubashi, Chiyoda-ku, Tokyo 101-8430, Japan*

(Received 7 February 2012; published 15 March 2012)

The spin coherence of an ensemble of electrons bound to fluorine donors in epitaxially grown ZnSe layers is studied by time-resolved pump-probe Kerr rotation. Long-lived spin dephasing with decay times up to $T_2^* = 33$ ns is found for a sample with a low fluorine concentration of 1×10^{15} cm^{-3} at cryogenic temperatures. The time is close to the limit set by nuclear-spin fluctuations, for which we measure a strength of 1.65 mT. We find T_2^* to be constant up to 40 K, with a strong drop for higher temperatures. The dephasing time also shortens with increasing fluorine concentration, indicating an interaction between the spins at different fluorine centers.

DOI: 10.1103/PhysRevB.85.121303 PACS number(s): 78.55.Et, 78.67.−n, 03.67.−a

Impurities in semiconductors promise a combination of the homogeneity of atomic systems with a controlled location in the solid state. The location can be controlled by doping or implantation of the impurities. In addition, impurities and the related bound charge carrier states can provide strong optical transitions and long-lived spin coherences. Among the presently investigated materials the impurities in silicon possess excellent homogeneity[1] and long coherence times[2] but are optically dark. Deep impurities in diamond, such as the nitrogen-vacancy (NV) centers, are bright[3] and particularly attractive as they provide robust spin coherence even at room temperature.[4] However, the fabrication of heterostructures such as high-Q microcavities with diamond is challenging. The impurities in GaAs-based semiconductors are also quite homogeneous, but the small binding energy of electrons to them makes a defined isolation and robust manipulation of single impurities rather difficult. Furthermore, it has been shown that the nuclear spins in III-V semiconductors cause fast decoherence of electron spins through a hyperfine interaction.[5]

We suggest that impurities in wide-gap II-VI semiconductors have a substantial potential to consolidate most of the advantages of such solid-state systems, because the direct band gap in II-VI materials offers efficient coupling to photons and integration of the impurities into the lattice does not lead to large inhomogeneities of the optical transitions. Most important may be, however, the low natural abundances of nonzero nuclear-spin isotopes in II-VI materials. The existence of zero nuclear-spin isotopes can be also isotopically purified to deplete nonzero nuclear spins.[6] This method has led to increased spin dephasing times in ZnO colloidal nanocrystals[7] and in silicon.[8] Finally, the ability to combine different II-VI materials with a small lattice mismatch to GaAs substrates provides advanced fabrication and nanostructuring techniques.

Particularly, fluorine is an attractive impurity in ZnSe, since it resembles a donor impurity when it replaces a selenium site in the ZnSe crystal.[9,10] The large electron binding energy of 29 meV allows thermal stability of donor-bound electrons.[11] The spin 1/2 of the fluorine nucleus with 100% natural abundance has the additional potential for a long-lived quantum memory because it could allow for schemes involving the transfer of electron-spin entanglement to the nuclear spin via double-resonance techniques.[12] In earlier experiments the indistinguishability of photons emitted from two independent excitons that are bound to distinct isolated fluorine impurities has been demonstrated.[13] Magnetospectroscopy studies of single impurities also confirm the possibility of creating a three-level optical λ system through the Zeeman splitting of the electron spin.[14,15] Despite all of the above-mentioned achievements, to the best of our knowledge, no studies of the spin coherent properties of fluorine donor electrons have been presented so far.

In this Rapid Communication we report time-resolved Kerr-rotation studies of the optically induced spin coherence in an ensemble of electrons bound to fluorine donors in ZnSe layers with various fluorine concentrations. We analyze the role of nuclei fluctuations and donor concentration on electron-spin dephasing and test the thermal stability of the coherence.

Three structures with homogeneously fluorine-doped ZnSe layers of thickness 70–100 nm are studied. The samples were grown by molecular-beam epitaxy on (001)-GaAs substrates on top of a thin buffer layer of ZnSe to define a clean interface for the II-VI/III-V heteroepitaxy. The applied fluorine fluxes correspond to doping concentrations of 1×10^{15}, 6×10^{17}, and 1×10^{18} cm^{-3} for samples A, B, and C, respectively. The fluorine concentration was obtained from capacitance-voltage curves of indium/nickel Schottky contacts with 300-μm diameter which were deposited by using optical lithography and a lift-off process. The ZnSe:F layers were grown on top of a 20-nm-thick $Zn_{1-x}Mg_xSe$ layer that prevents carrier diffusion into the lower band gap GaAs used as a substrate. The magnesium concentration of this layer was kept below 15% to maintain good crystal quality.

Figure 1 shows the reflectivity (red/light gray) and photoluminescence (PL) (gray shaded area) spectra for sample B. The reflectivity spectrum exhibits two strong resonances that correspond to the free-exciton complexes involving the heavy hole (HH) at 2.806 eV and the light hole (LH) at 2.818 eV. The splitting between the HH and LH excitons, which are degenerate in bulk materials, becomes prominent by the stress induced by the pseudomorph ZnSe lattice on top of GaAs.[16]

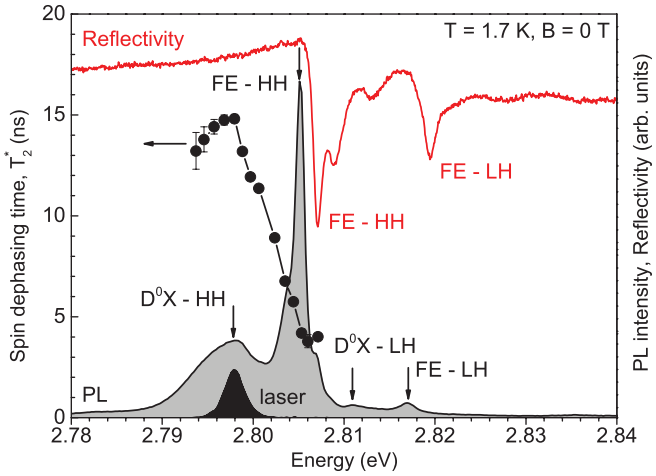

FIG. 1. (Color online) Spectroscopic study of ZnSe:F, sample B. The black line with the gray shaded area is a photoluminescence spectrum excited at 3.06 eV. The red (gray) line on top of the figure is a reflectivity spectrum measured with a halogen lamp. The solid circles give the dephasing time of donor-bound electrons measured by pump-probe Kerr rotation around zero magnetic field. The black shaded area shows the spectrum of the laser used in time-resolved experiments.

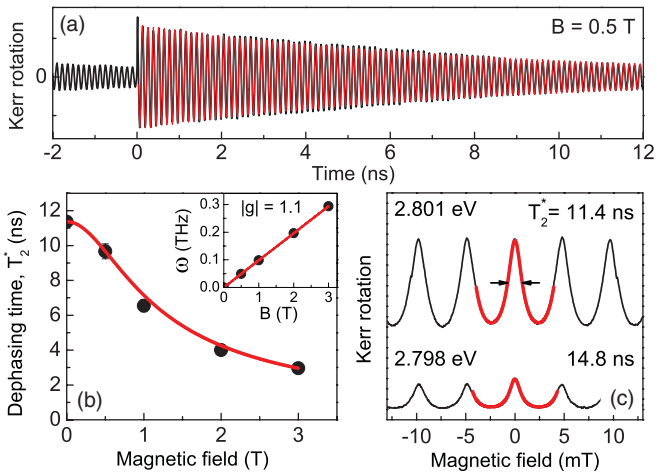

FIG. 2. (Color online) (a) Kerr rotation signal for sample B at $T = 1.7$ K. $P_{\text{pump/probe}} = 6/0.6$ W/cm^2 and 2.801 eV photon energy. (b) Spin dephasing time as a function of external magnetic field. The inset is the Larmor frequency dependence on the magnetic field (B) with a linear fit giving an electron g factor of 1.1 ± 0.1. (c) Resonant spin amplification signal measured at 2.801 eV. The width of the central peak gives $T_2^* = (11.4 \pm 0.1)$ ns. The bottom curve is measured at 2.798 eV and leads to (14.8 ± 0.2) ns spin dephasing time. The red (gray) curves are fits to the data using Eq. (1) (see the text).

Additional peaks on the higher-energy side of the HH and LH peaks can be assigned to the quantization of exciton polaritons in thin ZnSe films.[17]

The PL spectrum demonstrates a peak pattern where each feature can be assigned to different exciton complexes. Labels mark the transitions, with FE being the free exciton and D^0X the donor-bound excitons containing HH or LH. The broadening of transitions is related to the strain in the structure.[9] The PL emission was also analyzed by a synchroscan streak camera with an S20 photocathode giving recombination times of (210 ± 40) ps for D^0X and (30 ± 3) ps for FE-HH. Similar PL decay times were reported in Ref. 9.

To obtain insight into the electron-spin coherence we apply time-resolved pump-probe Kerr rotation (KR). Both the pump and probe have the same photon energy, taken from a Ti:sapphire laser emitting pulses at a rate of 75.75 MHz (corresponding to 13.2-ns pulse separation). The laser pulse duration is 1 ps. The laser frequency is doubled by a BBO (beta barium borate) crystal to convert the Ti:Sa range of photon energies from about 1.25–1.7 to 2.5–3.4 eV. The sample is placed in a superconducting split-coil optical magnet that allows one to generate fields up to 3 T. The sample temperatures can be varied from 1.7 to 300 K.

After excitation of the sample along the growth axis **z** with the circularly polarized pump pulse, the reflection of the linearly polarized probe is analyzed with respect to the angle of polarization rotation as a function of delay between the pump and probe. To reduce the possibility of dynamic nuclear polarization we use a photoelastic modulator for a pump helicity modulation at 84 kHz.[18] A characteristic KR signal measured in a magnetic field of $B = 0.5$ T applied normal to **z** (Voigt geometry, $\mathbf{B} \perp \mathbf{z}$) with a laser energy at 2.801 eV is shown in Fig. 2(a). We choose this energy because the KR amplitude is maximum at this spectral position.

The long-lived, nanosecond-lasting KR signal arises from the resident electrons localized at the fluorine donor centers. The frequency and decay time of this signal are measures of the average g factor and the spin dephasing time T_2^* in the excited spin ensemble of spins. To determine these parameters we use the fitting function for the data, $f_{\text{KR}}(t) \propto \exp(-t/T_2^*)\cos(\omega t)$, which gives the best-fit results. Here $\omega = g\mu_B B/\hbar$ is the Larmor frequency, with the Bohr magneton μ_B and the Planck constant $\hbar$. A corresponding fit is shown by the thin red (gray) curve on top of the measured data in Fig. 2(a).

The magnetic field dependence of the spin dephasing time T_2^* is shown in Fig. 2(b). It can be described by the following function:

$$T_2^*(B) = \hbar/\sqrt{(\Delta g \mu_B B)^2 + (g\mu_B \Delta B)^2}, \qquad (1)$$

with fit parameters $\Delta g = 0.001$ being the spread of g factors, which is about 0.1% of the g value, and $\Delta B = 0.9$ mT representing the limiting factor at low fields. We note that Δg was similar in all three samples.

For fields $B > 0.5$ T the spin dephasing time decreases with B, following a $1/B$ dependence. This well-known behavior arises from the dispersion of electron g factors excited by the laser of finite spectral width, which leads to a spread of Larmor frequencies $\Delta\omega = \Delta g \mu_B B/\hbar$ that increases with magnetic field. At low fields the dephasing time saturates at a value, which is determined by intrinsic processes in the system, such as spin-orbit interactions or the nuclear-spin fluctuations, as discussed later in this Rapid Communication.

As one can see from the Fig. 2(a), the amplitude of the KR signal does not decay completely within the pulse separation time of the laser ($T_R = 13.2$ ns). As a result, the next pump pulse excites spins before the previously excited spin polarization has completely dephased. This leads to

some uncertainty in evaluating T_2^*. Hence, we also apply a complementary technique called resonant spin amplification (RSA).[19] For that purpose we fix the probe pulse delay at $\Delta t = -50$ ps, shortly before the next pump pulse, and scan the magnetic field. The total spin polarization is then resonantly enhanced whenever $\omega(B)T_R$ is a multiple integer of 2π, a condition that is met periodically when ramping the applied magnetic field—see Fig. 2(c). To extract the spin dephasing time around zero field from these data, we fit the measured signal by the following form, using T_2^* as the only free-fitting parameter:

$$f_{\mathrm{KR}}(B) \propto e^{-\frac{\Delta t + T_R}{T_2^*}} \frac{\cos(\omega \Delta t) - e^{\frac{T_R}{T_2^*}} \cos[\omega(\Delta t + T_R)]}{\cos(\omega T_R) - \cosh(T_R/T_2^*)}. \quad (2)$$

The solid circles in Fig. 1 give the spectral dependence of the spin dephasing time as measured by the RSA method. For times shorter than 8 ns we have used the time-resolved KR signal to extract the decay constant. As one can see, the dephasing time grows for lower energies and reaches a maximum at a spectral position around the donor-bounded exciton, D^0X, energy. Here it saturates and stays nearly constant for further decreasing energy. An exemplary RSA spectrum for the maximal $T_2^* = 14.8$ ns is shown at the bottom of Fig. 2(c).

To evaluate the role of nuclear-spin fluctuations in the electron-spin dephasing on the time scales observed here, we use the following equation:[20,21]

$$T_2^* = \hbar \sqrt{\frac{3N}{2\sum_j I_j(I_j+1)A_j^2 y_j}}, \quad (3)$$

where the sum is running over the nuclear spins I_j of isotope j with the abundance y_j. A_j is the hyperfine constant and N the total number of nuclei which overlap with the wave function of an electron localized on a fluorine donor. $N \approx 21\,000$ is estimated from the ratio of the Bohr volume $V_B = 4/3\pi a_B^3 = 470$ nm^3 (using $a_B = 4.825$ nm—see below) and the single-cell volume containing eight atoms of ZnSe. For the single cell in tetragonal strained ZnSe we use $a_z = 0.56686$ nm and $a_{x,y} = 0.5653$ nm,[22] and the Bohr radius for a shallow donor is estimated by $1.5\varepsilon_{\mathrm{ZnSe}} 0.053/(m_e^{\mathrm{eff}}/m_e)$ nm. Here $\varepsilon_{\mathrm{ZnSe}} = 8.8$ is the dielectric constant of ZnSe, the 0.053 nm is the Bohr radius of hydrogen, and $m_e^{\mathrm{eff}} = 0.145 m_e$ is the effective electron mass. For ZnSe we find from literature: ^{67}Zn ($I = 5/2$, $y = 4.11\%$) $A_{\mathrm{Zn}} = 3.7$ μeV,[7] and ^{77}Se ($I = 1/2$, $y = 7.58\%$) $A_{\mathrm{Se}} = 33.6$ μeV.[21] Using Eq. (3) we get as an estimate for $T_2^* = 14$ ns.[23] Based on such a simple estimation, this value is quite close to the measured spin dephasing time of 14.8 ns—see Fig. 2(c).

The fluorine nuclei ^{19}F [$I = 1/2$, $y = 100\%$, and $A_{\mathrm{F}} \approx 200$ μeV (Ref. 24)] replaces selenium and also contributes to spin dephasing. For a fluorine density of 1×10^{18} cm^{-3} the average distance between neighboring fluorine atoms is larger than the Bohr radius of bound electrons. Therefore, compared to the number of nonzero nuclear spins within the Bohr volume ($\approx$430 for ^{67}Zn and $\approx$790 for ^{77}Se) the interaction with a single ^{19}F atom should be very small. We estimate the effect of fluorine by using Eq. (3) with an effective fluorine abundance $y^{\mathrm{eff}} = 1/N = 0.0048\%$ and get $T_2^* = 13.9$ ns. It corresponds to less than 1% of spin dephasing time reduction compared to the time estimated without a fluorine contribution.

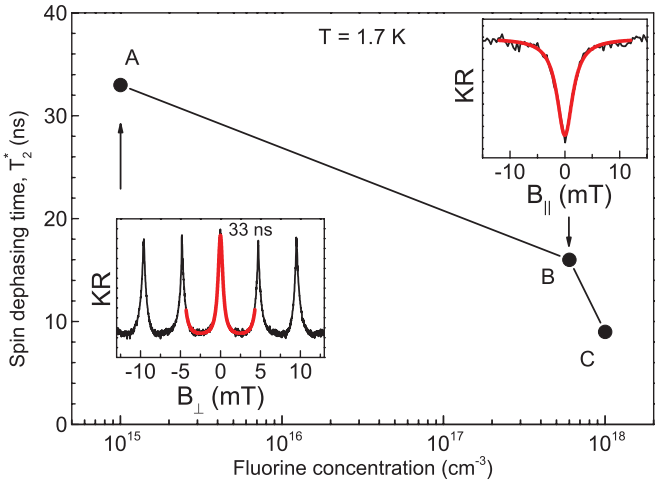

FIG. 3. (Color online) Spin dephasing time T_2^* measured at the D^0X energy (2.798 eV) vs fluorine concentration in the corresponding samples. The line is a guide to the eye. Left-hand inset: RSA measurement ($\mathbf{B} \perp \mathbf{z}$) for sample A with the red (gray) curve being a fit using Eq. (2). Right-hand insert: Magnetic field dependence ($\mathbf{B} \parallel \mathbf{z}$) of the electron-spin polarization for sample B and fit by Eq. (4).

To support the estimation we measure directly the nuclear-spin fluctuation. For this purpose, experimental conditions similar to those for RSA are used with the probe pulse fixed at $\Delta t = -50$ ps delay position, but the scanned magnetic field is applied in the Faraday geometry ($\mathbf{B} \parallel \mathbf{z}$). The inset in the top right-hand corner of Fig. 3 demonstrates the result of this measurement for sample B. We observe an increase in the spin polarization for higher fields that can be interpreted as a suppression of the influence of all components of nuclear-spin fluctuations by the external magnetic field. The width of the observed dip can be used as a direct measure of these fluctuations, which are commonly described by an average hyperfine magnetic field B_f defined by[25]

$$f_{\mathrm{KR}}(B) = f_0 \left[1 - \frac{2/3}{1 + (B/B_f)^2}\right], \quad (4)$$

with $B_f = 1.65$ mT being the half width at half minimum (HWHM) of the dip. Therefore the electron-spin dephasing time caused by the field B_f is $T_2^* = 2\sqrt{3}\hbar/(g\mu_B B_f) = (20 \pm 1)$ ns.[25] This value is close to the $T_2^* = 14$ ns from Eq. (3), giving additional support for our above estimation and the nuclear-spin involvement in the spin dephasing. The nature of the electron-nuclear interaction does require deeper investigations and is out of the scope of this Rapid Communication.

Figure 3 shows the longest T_2^* data measured for the three studied samples as functions of the corresponding fluorine concentration. As in the case of sample B, shown in Fig. 2(c), the longest time is measured at the donor peak position, D^0X (2.798 eV). The observed dependence demonstrates that an increase in fluorine concentration accelerates the electron-spin dephasing. The reason for this could be the increased probability of scattering events between neighboring electrons or electron jumps between closely spaced donor centers.

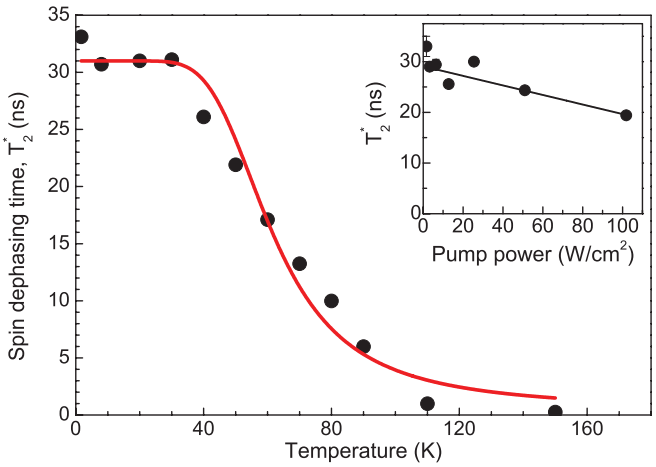

FIG. 4. (Color online) Temperature dependence of spin dephasing time T_2^* measured at the D^0X energy for sample A. $P_{\text{pump/probe}} = 6/0.6$ W/cm^2. The solid (red) line is a fit by Eq. (5). The inset gives the pump power dependence of T_2^*. The solid line is a guide to the eye.

Finally, we use sample A to test the spin dephasing as a function of laser power and temperature. First, the inset in Fig. 4 demonstrates that the pump power does not have a large impact on the dephasing time over a broad range of powers. This is valid for all samples and indicates strong localization of the electrons. For support we measure the temperature dependence of the spin dephasing time—see Fig. 4. Here the laser energy is shifted according to the expected band-gap shift by using the equation $E(T)[\text{eV}] = 2.798–5.9 \times 10^{-4} T[\text{K}]^2/(T[\text{K}] + 197)$.[16] A fit to the data is given by a function describing thermal activation from the ground state with a relaxation time (T_g) to an excited state with relaxation time (T_e):

$$\frac{1}{T_2^*} = \frac{1}{T_g} + \frac{1}{T_e} \exp\left[-\frac{E_a}{k_B T}\right]. \quad (5)$$

E_a is the activation energy of the donor-bound electron and k_B is the Boltzmann constant. The fit gives $T_g = (31 \pm 1)$ ns, $T_e = (220 \pm 3)$ ps, and $E_a = (27 \pm 1)$ meV. The T_e falls into the range of measured exciton recombination times (see above) and E_a coincides well with the fluorine-bound electron activation energy of 29.3 ± 0.6 meV.[11]

To conclude, we have demonstrated high fluorine-bound electron stability and measured spin dephasing times in the 10-ns range. The dephasing time limitation at low fluorine concentrations is caused by the nuclear isotopes with nonzero spin, while for higher fluorine concentrations ($n_F > 10^{15}$ cm^{-3}) the interaction between neighbor electrons accelerates the spin dephasing.

This research was supported by the Deutsche Forschungsgemeinschaft, the NTT Basic Research Laboratories, the Commissioned Research of National Institute of Information and Communications Technology (NICT), by the Ministry of Education, Culture, Sports, Science and Technology (MEXT), and through the Funding Program for World-leading Innovative Research and development on Science and Technology (FIRST).

*alex.greilich@udo.edu
†pawlis@stanford.edu

[1] A. Yang, M. Steger, D. Karaiskaj, M. L. W. Thewalt, M. Cardona, K. M. Itoh, H. Riemann, N. V. Abrosimov, M. F. Churbanov, A. V. Gusev *et al.*, Phys. Rev. Lett. **97**, 227401 (2006).
[2] A. M. Tyryshkin, S. A. Lyon, A. V. Astashkin, and A. M. Raitsimring, Phys. Rev. B **68**, 193207 (2003).
[3] P. Neumann, N. Mizuochi, F. Rempp, P. Hemmer, H. Watanabe, S. Yamasaki, V. Jacques, T. Gaebel, F. Jelezko, and J. Wrachtrup, Science **320**, 1326 (2008).
[4] G. Balasubramanian, P. Neumann, D. Twitchen, M. Markham, R. Kolesov, N. Mizuochi, J. Isoya, J. Achard, J. Beck, J. Tissler *et al.*, Nat. Mater. **8**, 383 (2009).
[5] S. M. Clark, K.-M. C. Fu, Q. Zhang, T. D. Ladd, C. Stanley, and Y. Yamamoto, Phys. Rev. Lett. **102**, 247601 (2009).
[6] R. Lauck and E. Schönherr, J. Cryst. Growth **197**, 513 (1999).
[7] K. M. Whitaker, S. T. Ochsenbein, A. L. Smith, D. C. Echodu, B. H. Robinson, and D. R. Gamelin, J. Phys. Chem. C **114**, 14467 (2010).
[8] S. D. Sarma, R. de Sousa, X. Huc, and B. Koillerd, Solid State Commun. **133**, 737 (2005).
[9] A. Pawlis, K. Sanaka, S. Götzinger, Y. Yamamoto, and K. Lischka, Semicond. Sci. Technol. **21**, 1412 (2006).
[10] L. S. dos Santos, W. G. Schmidt, and E. Rauls, Phys. Rev. B **84**, 115201 (2011).
[11] J. L. Merz, H. Kukimoto, K. Nassau, and J. W. Shiever, Phys. Rev. B **6**, 545 (1972).
[12] S. C. Benjamin, D. E. Browne, J. Fitzsimons, and J. J. L. Morton, New J. Phys. **8**, 141 (2006).
[13] K. Sanaka, A. Pawlis, T. D. Ladd, K. Lischka, and Y. Yamamoto, Phys. Rev. Lett. **103**, 053601 (2009).
[14] K. D. Greve, S. M. Clark, D. Sleiter, K. Sanaka, T. D. Ladd, M. Panfilova, A. Pawlis, K. Lischka, and Y. Yamamoto, Appl. Phys. Lett. **97**, 241913 (2010).
[15] Y. M. Kim, D. Sleiter, K. Sanaka, Y. Yamamoto, J. Meijer, K. Lischka, and A. Pawlis, Phys. Rev. B **85**, 085302 (2012).
[16] R. J. Thomas, B. Rockwell, H. R. Chandrasekhar, M. Chandrasekhar, A. K. Ramdas, M. Kobayashi, and R. L. Gunshor, J. Appl. Phys. **78**, 6569 (1995).
[17] A. Tredicucci, Y. Chen, F. Bassani, J. Massies, C. Deparis, and G. Neu, Phys. Rev. B **47**, 10348 (1993).
[18] D. R. Yakovlev and M. Bayer, *Spin Physics in Semiconductors* (Springer, Berlin, 2008), Chap. 6, pp. 135–175.
[19] J. M. Kikkawa and D. D. Awschalom, Phys. Rev. Lett. **80**, 4313 (1998).
[20] I. A. Merkulov, A. L. Efros, and M. Rosen, Phys. Rev. B **65**, 205309 (2002).
[21] M. Syperek, D. R. Yakovlev, I. A. Yugova, J. Misiewicz, I. V. Sedova, S. V. Sorokin, A. A. Toropov, S. V. Ivanov, and M. Bayer, Phys. Rev. B **84**, 085304 (2011); **84**, 159903(E) (2011).

[22] A. Pawlis, T. Berstermann, C. Brüggemann, M. Bombeck, D. Dunker, D. R. Yakovlev, N. A. Gippius, K. Lischka, and M. Bayer, Phys. Rev. B **83**, 115302 (2011).

[23] Using a similar estimation approach for bulk GaAs and CdTe we are getting spin dephasing times of 5 ns for both systems. Spin dephasing times $T_2^* = 1$ ns (Ref. 5) and 2.8 ns (Ref. 26) in an ensemble of Si donors in GaAs were reported.

[24] J. R. Morton and K. F. Preston, J. Magn. Res. **30**, 577 (1978).

[25] M. Y. Petrov, I. V. Ignatiev, S. V. Poltavtsev, A. Greilich, A. Bauschulte, D. R. Yakovlev, and M. Bayer, Phys. Rev. B **78**, 045315 (2008).

[26] M. Römer, H. Bernien, G. Müller, D. Schuh, J. Hübner, and M. Oestreich, Phys. Rev. B **81**, 075216 (2010).